Journal of Physical Sciences, Vol. 16, 2012, 209-216
ISSN: 0972-8791, www.vidyasagar.ac.in/journal
Published on 31 December 2012

Synthesis and Properties of Polyaniline Samarium Nanocomposite

K.Gupta[1], P.C. Jana[2] and A.K.Meikap[1]

[1]Department of Physics, National Institute of Technology, Mahatma Gandhi Avenue Durgapur-713209, West Bengal, India.
[2]Department of Physics and Technophysics, Vidyasagar University Midnapore 721102, West Bengal, India.
Email: pareshjana@rediffmail.com

Received October 19, 2012; accepted December 18, 2012

ABSTRACT

The main objective of this investigation is to study the effect of samarium nanoparticles on the optical and electrical transport properties of polyaniline. Polyaniline-samarium nanocomposite has been prepared by chemical oxidative polymerization of aniline in presence of samarium nanoparticles. Average grain size lies in the range 30-40 nm. A red shift in the optical absorption is obtained. Temperature and magnetic field affect the electrical transport properties of our samples. Conductivity and magnetoconductivity have been increased with temperature.

Keywords*:* Polyaniline, Samarium, Optical, Electrical transport

I. Introduction

Nanomaterials have excellent optical and electronic properties and these interesting properties are being used in various electronic and optical devices. [1-2]. In recent years, the electrical and optical properties of a metal nanoparticles embedded in a dielectric medium have been a subject of immense interest. Conducting polymers are being used as dielectric medium. Conducting polymers have extended π - conjugation with single- and double-bond alteration along the polymer chain. They are semiconductors with low charge carrier mobility. Conductivity of these polymers can be increased up to the metallic range by way of doping [3-4]. It shows interesting tunable properties like electrical, magnetic, optical, and chemical properties. Hence these conducting polymers are widely used in different technological applications like electromagnetic interference (EMI) shielding, rechargeable batteries, electrodes, Light emitting diodes, sensors, corrosion protection coatings, and microwave absorption [5-10]. Polyaniline is a conducting

polymer which can be used as a dielectric medium. Preparation of polyaniline from aniline, a very cheap monomer, is very simple and its environmental and thermal stability is very good in comparison to other conducting polymers. Its conductivity is also very high compare to others and it exhibits good electrical, optical, magnetic and chemical properties [11-13]. Hence we have taken polyaniline in this investigation. Rare earth elements have unique optical, magnetic and electrical properties. Thus we have chosen samarium.

We have prepared polyaniline-samarium nanocomposite by chemical oxidative polymerization of aniline in presence of samarium nanoparticles. Samples are characterized by scanning electron microscope (SEM), X-ray diffractometer (XRD), uv visible spectroscopy. Standard four-probe method has been used to measure the electrical conductivity. D.c resistivity is measured in the temperature range $77 \leq T \leq 300$K in presence and absence of magnetic field using pellet of individual samples. Enhancement of both optical and electrical properties is observed. Thus the nanocomposite is of great importance.

2. Sample preparation and experimental technique

2.1. Synthesis

Aniline (MERCK) has been distilled for two times under reduced pressure to get a colourless distillate. Samarium nitrate (MERCK), ammonium peroxodisulphate (APS, MERCK), nitric acid and acetone required for this investigation is taken from local market. The typical synthetic process for the preparation of Polyaniline-samarium nanocomposite is as follows: Equal volume of acidified (0.2M HNO_3) aqueous 1mM aniline solution is mixed with 1 mM samarium nitrate solution and the mixture is stirred slowly to prepare homogeneous solution. Ice cooled 0.5 M APS solution is used in this investigation and added drop wise under continuous magnetic stirring. A green coloured solution is obtained which is left in refrigerator at rest for 24 hours to complete the polymerization process. A solid mass is obtained on centrifugation at 10000 rpm for an hour. It is washed with acetone and double distilled water to remove monomer, oligomers and excess oxidant until the filtrate become colourless. Samples are dried in an oven at 30^0C for overnight. For the comparison purposes we have prepared four samples using 0, 1, 5 and 10 mM samarium nitrate solution and they are marked as PS_0, PS_1, PS_5 and PS_{10} respectively.

2.2. Characterization

Morphology of samples is obtained by using a Scanning electron microscope (SEM). The phase identification is performed by Rigaku mini-flex-II desktop X-ray diffractometer (XRD) with nickel filter Cu k_α radiation (λ = 1.54 Å) in 2θ range from 20 to 90^0. The Uv-vis spectrum of the samples is taken by a double beam spectrophotometer (U-1700 Shimadzu) using dimethyl sulphoxide (DMSO) as a solvent. Standard four-probe method has been used to measure the dc conductivity and it is measured in the temperature range $77 \leq T \leq 300$K in presence and absence of magnetic field using pellet of individual samples.

3. Result and discussion

3.1. Morphology

SEM micrograph of polyaniline-samarium nanocomposite (PS_{10}) is shown in Fig.1. Granular morphology is seen from the micrograph. The grains present in the matrix are the composite of polyaniline with samarium nanoparticles that adsorbed on polyaniline matrix for the strong affinity of samarium nanoparticles for nitrogen atom of polyaniline. Diameter of the grains observed from the micrograph is in the range of 30-40 nm. Grains are well resolved and almost circular in shape.

3.2. Structural characterization

Room temperature XRD analysis is done to predict the crystal structure of polyaniline (PS_0) and its nanocomposite with samarium (PS_{10}). Fig.2 shows XRD pattern. The spectrum of PS_0 shows that it has no characteristic peak excluding a hump near $2\theta = 25.5^0$ which indicates amorphous nature of polyaniline. PS_{10} shows characteristic peaks at $2\theta = 30.8$, 34.0, 50.4 and 60.27^0 which are due to Bragg's reflections from (009), (015), (110), (119) planes of the hexagonal phase (Joint Committee on Powder Diffraction Standard no-06-0419) respectively. Hump at $2\theta = 25.5^0$ is of polyaniline for regular repetition of monomer unit. Hence crystalline behavior of the nanocomposite is due to the presence of samarium in the polyaniline matrix. Average grain size obtained using Scherrer's formula is 40 nm.

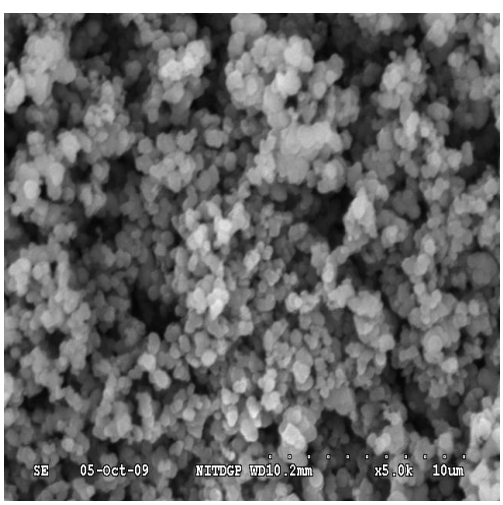

Figure 1: SEM micrograph

3.3. Optical property

Optical absorption spectrums of polyaniline (PS_0) and polyaniline-samarium nanocomposite (PS_1, PS_5, PS_{10}) are presented in Fig.3. Spectrums are taken for the same concentration (10 mg/100 ml DMSO) of each sample at room temperature. π-π^* transition in the benzenoid rings of polyaniline gives an absorption band at 320-

330 nm and the quinoid rings of polyaniline gives an exciton absorption band (n-π^*) at 610-620 nm. Erdem et al and Shihai et al obtained similar type of observation [14-15]. In polyaniline-samarium nanocomposite there occurs a red shift of the absorption bands. Shifting of the absorption band due to π-π^* transition in the benzenoid rings towards the wave length 330-350 nm and exciton absorption band

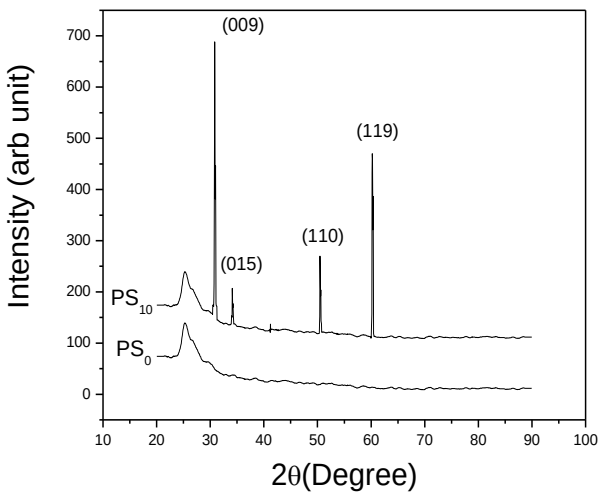

Figure 2: XRD pattern

of the quinoid ring towards the wave length 590-600 nm with low intensity are obtained. This red shift may be due to the interaction of samarium nanoparticles with amine and imine units of polyaniline causing changes in the electronic band. The red shift of the composite also indicates that the energy required for π-π^* and n-π^* transition in nanocomposite requires lower amount of energy than in case of polyaniline. Peak at 420 nm may be due to the presence of samarium nanoparticles in the composite. The optical absorption is calculated using the equation $\alpha h\nu = A(h\nu - E_g)^n$, where E_g, α, ν, A are the band gap, absorption coefficient, frequency, constant respectively and n can take values of 0.5, 1.5, 2 and 3 depending on the mode of transition. [16] Here n = 0.5 offers the best fit for the optical absorption data of polyaniline and polyaniline-samarium nanocomposites, lending support to the allowed direct band transition of the materials. In order to get the idea about band gap, a plot of $(\alpha h\nu)^2$ versus $h\nu$ has been done (not shown in the manuscript). Then the band gap has been extracted by extrapolating the straight portion of the graph on $h\nu$ axis at $\alpha = 0$ and those are 2.68, 2.37, 2.14, 2.01 eV for PS_0, PS_1, PS_5 and PS_{10} respectively. Conductivity of polyaniline increases in presence of samarium nanoparticles due to the decrease in band gap and this type of behavior is also observed in the electrical conductivity measurements.

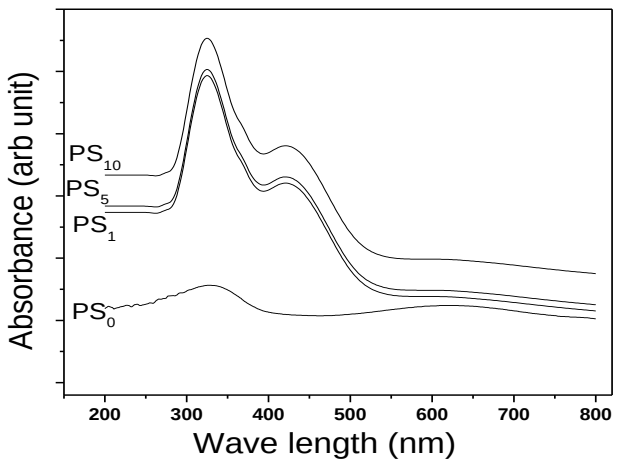

Figure 3: Uv-vis spectrum

3.4. Electrical Transport Mechanism

Dc conductivities of the samples are measured to interpret the influence of samarium nanoparticles on dc conductivity of polyaniline in the temperature range $77 \leq T \geq 300K$. Semiconducting behavior is obtained in the temperature range of investigation. The conductivity of different samples varies in between 10^{-8} to 10^{-5} $\Omega^{-1}m^{-1}$ with temperature. Introduction of Sm nanoparticles in polyaniline matrix may be the cause of increase in conductivity of the nanocomposites. Efficiency of charge transfer between polyaniline chains and Sm nanoparticles occurs more with increase in temperature and as a result conductivity increases with increase in temperature. Mott's variable range hopping (VRH) theory will be the most suitable to explain the true charge transport mechanism. [17] According to this theory, the conductivity is given by

$$\sigma(T) = \sigma_o (T_{Mott}/T)^{1/2} \exp[-(T_{Mott}/T)^{\gamma}] \quad (1)$$

$$T_{Mott} = \frac{16}{k_B N(E_F) L_{loc}^3} \quad (2)$$

where γ is the VRH exponent which determines the dimensionality of the medium. A possible value of γ is ¼, 1/3 and ½ for three, two and one dimensional system respectively. σ_o is the conductivity at infinite temperature, T_{Mott} denotes the Mott characteristic temperature, k_B is the Boltzmann constant, $N(E_F)$ is the density of states at Fermi level and L_{loc} is the localization length respectively. A graph of $\ln[T^{1/2}\sigma(T)]$ and $T^{-1/4}$ has been plotted [given in Fig.4] for all the samples and a linear variation is obtained which indicates three dimensional charge transport mechanism in the samples. Values of T_{Mott} lie in between 10^7 and 10^9K for our different samples. We have tried to know the effect of magnetic field (upto 1Tesla) on dc conductivity of our samples. Fig.5 shows the variation of magnetoconductivity

ratio at T = 300K with varying magnetic field for all the samples. A positive magnetoconductivity is obtained for our samples. The measured magnetoconductivity data can be explained by the orbital magnetoconductivity theory [18-20]. This orbital magnetoconductivity theory (forward interference model) predicts the forward interference among the random paths in the hopping process between the two sites spaced at a distance equal to optimum hopping distance resulting in positive magnetoconductivity and can be expressed as

$$\frac{\sigma(B,T)}{\sigma(0,T)} = 1 + \frac{\frac{C_{sat}B}{B_{sat}}}{1+\frac{B}{B_{sat}}} \tag{3}$$

where C_{sat} is a temperature independent parameter and $B_{sat} = 0.7(h/e)(8/3)^{3/2}(1/L_{loc}^{2})(T/T_{Mott})^{3/8}$. Since at 300K, the investigated samples show positive magnetoconductivity, the measured data is analyzed with the help of orbital magnetoconductivity theory. The different points in Fig.5 are the experimental data for different samples and the solid lines are the theoretical best fit obtained from Eq.3, taking C_{sat} and B_{sat} as fitting parameters. The localization length L_{loc} can be obtained from the fitting parameter B_{sat} and the value of the T_{Mott}. The variation of dc magnetoconductivity of the samples at different temperature is shown in the inset of Fig.5 and can be explained in terms of orbital magnetoconductivity theory. With increasing temperature, the average hopping length increases due to which, there is an enhancement of magnetoconductivity with increasing temperature. The average hopping length (R_{hop}) can be calculated by the relation

$$R_{hop} = (3/8)(T_{Mott}/T)^{1/4} L_{loc} \tag{4}$$

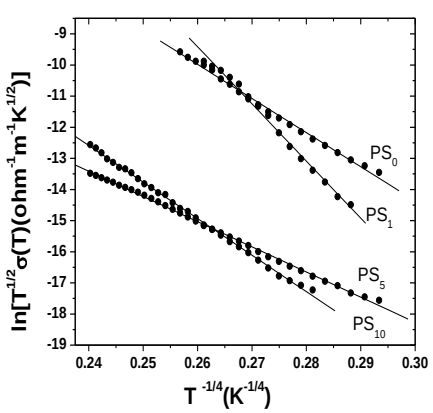

Figure 4: Temperature variation of conductivity

The average hopping length increases from 0.08 nm to 0.20 nm with the increase in temperature. Thus, the enhancement of magnetoconductivity with temperature can be explained in terms of enhancement of average hopping length with temperature.

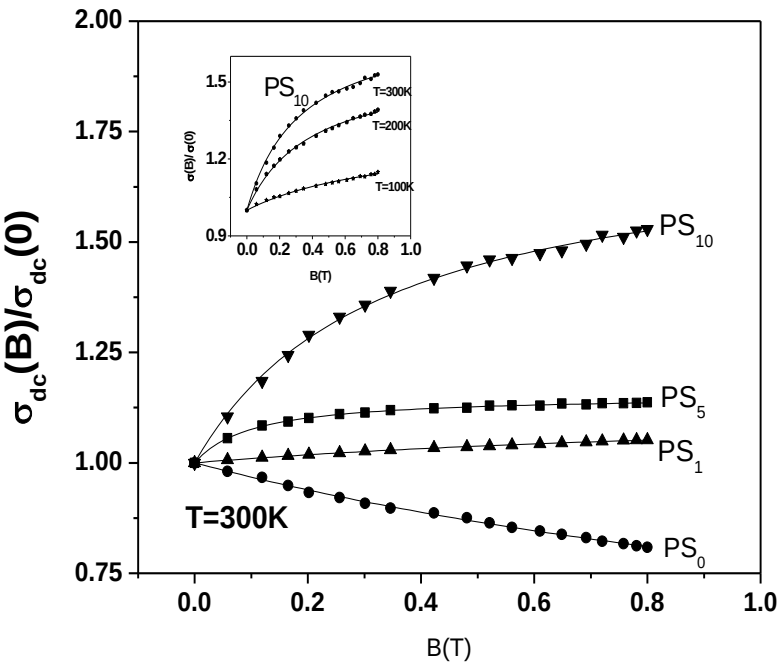

Figure 5: Variation of magneto conductivity with samples and temperature

4. Conclusion

Polyaniline-samarium nanocomposite has been prepared by in situ chemical oxidative polymerization of aniline. A red shift in the optical absorption is obtained. Conductivity and magnetoconductivity are enhanced with temperature and magnetic field.

REFERENCES

1. A. P. Alivisatos, Science, 271 (1996) 933.
2. R. J. Ellingson, M. C. Beard, J. C. Johnson, P. Yu, O. I. Micic, A. J. Nozik, A. Shabaev and A. L. Efros, Nano Lett., 5 (2005) 865.

3. K. Lee, S. Chio, S.H. Park, A. J. Heeger, C. Loo, S. H. Lee, Nature letters 441/4, (2006) 65.
4. D.Chaudhuri, A. Kumar, I. Rudra, D. D. Sharma, Adv. Mater., 13 (2001) 1548.
5. J. C. Aphesteguy, P. G. Bercoff,s.e. Jacobo, Physica, B 398 (2007) 200.
6. H. Naarman, Science and Application of Conducting Polymers Adam Hilger; Bristol, 1991.
7. J. Joo, A.J.Epstein, Appl. Phys. Lett., 65 (1994) 2278.
8. J.A. Osaheni,A.S. Jenekhe, H. Vanherzeele,J.S. Meth, Y. Sun, A.G. MacDiarmid, J Phys Chem, 96 (1992) 2830.
9. Z. Hau, J. Shi, L. Zhang, M. Ruan, J. Yan, Adv. Mater., 14 (2002) 830.
10. N. Asim, S. Radiman, M.A.Bin Yarmo, Mater. Lett., 62 (2008) 1044.
11. Li, Y. Gao, X. Zhang, J. Gong, Y. Sun, X. Zheng, and L. Qu, Mater. Lett., 62, (2008) 2237.
12. S. K. Pillalamarri, F. D. Blum, A. T. Tokuhiro, M. F. Bertino, Chem. Mater. 17(2005) 5941.
13. Y. Haba, E. Segal, M. Narkis, G. I. Titelman, A. Siegmann, Synth. Met., 110 (2000) 189.
14. E. Erdem, M. Karakisla, and M. Sacak, Euro. Polym. Journal, 40 (2004) 785.
15. D. Shihai, M. Hui, and W Zhang, J. Appl. Polym. Sci., 109 (2008) 2842.
16. S. Subramanian, and D. P. Padiyan, Mater. Chem. and Phys., 107 (2008) 392.
17. N. F. Mott and E. A. Davis, Electronic Processes in Non-Crystalline Materials, (Clarendon, Oxford, 1971).
18. V. L. Nguyen, B. Z. Spivak, B. I. Shklovskii, JETP Lett., 41 (1985) 42.
19. V. L. Nguyen, B. Z. Spivak, B. I. Shklovskii, Sov. Phys. JETP, 62 (1985) 1021.
20. U. Sivan, O. Entin-Wohiman, Y. Imry, Phys. Rev. Lett., 60 (1988) 1566.